Coordination Chemistry Reviews 470 (2022) 214705

Contents lists available at ScienceDirect

Coordination Chemistry Reviews

journal homepage: www.elsevier.com/locate/ccr

Review

# Metal-organic ion transport systems

Kylie Yang [1], Hiral A. Kotak [1], Cally J.E. Haynes *

*Chemistry Department, University College London, 20 Gordon Street, London WC1H 0AJ, UK*

ARTICLE INFO

*Article history:*
Received 30 March 2022
Accepted 28 June 2022
Available online 25 July 2022

*Keywords:*
Ion transport
Coordination complex
Membranes
Stimuli-responsive
Supramolecular

ABSTRACT

The design of synthetic membrane transporters for ions is a rapidly growing field of research, motivated by the potential medicinal applications of novel systems. Metal-organic coordination complexes provide access to a wide range of geometries, structures and properties and their facile synthesis and tunability offer advantages in the design of ion transport systems. In this review, the application of metal-organic constructs as membrane-spanning channels and ion carriers are explored, and the roles of the metal coordination complexes within these functional assemblies are highlighted.


**Contents**



## 1. Introduction

The transport of ions through biological membranes is vital to life, and ion transport has diverse roles that encompass the storage of cellular energy in the form of electrochemical gradients, cell signalling and communication, fluid balance, and pH regulation [1]. Consequently, cells contain several unique ionic environments that are compartmentalised within the plasma membrane, membrane-bound organelles, endosomes and vesicles. Because ions are impermeable to lipid membranes, ion transport must be mediated via the highly regulated action of membrane-bound proteins, such as ion pumps, which transport ions against an electrochemical gradient using active processes, and ion channels which provide a membrane-spanning pore through which ions can diffuse [2].

While most examples of ion transport in biological systems occur via the action of proteins, ion transport can also be mediated by synthetic constructs. Such synthetic ion transporters can operate via two main mechanisms; mobile carriers can bind to and increase the hydrophobicity of ions to allow them to passively diffuse through the lipid bilayer, whilst channels insert into the membrane and provide a pore through which ions can move. Due to the need for carriers and channels to interact with both the lipid bilayer and the ion of interest, they need to contain both lipophilic and polar properties.

A combination of several techniques are currently used to predict the structure of an active transporter within a lipid bilayer,

* Corresponding author.
*E-mail address:* cally.haynes@ucl.ac.uk (C.J.E. Haynes).
[1] These authors contributed equally.

https://doi.org/10.1016/j.ccr.2022.214705
0010-8545/

however it is important to note that the absolute conformation of molecules within the membrane is difficult to determine. Structural studies in solution and crystallography in the solid state can only indicate potential structures of transporters in a membrane. Therefore, authors often propose the structures of the active ionophores based on studies outside bilayers and indirect evidence from transport assays. These transport assays are often conducted in synthetic vesicles, and the concentration of a certain ion can be monitored via use of a fluorescent or colorimetric indicator e.g., 8-hydroxypyrene-1,3,6-trisulfonic acid (HPTS) for $H^+$, and lucigenin for $Cl^-$, or ions can be monitored via ion selective electrode readings. Additionally, patch clamp measurements or phospholipid bilayer conductance (PBC) measurements can be used to observe channel opening and closing events in patched sections of a curved bilayer, such as a cell membrane/vesicle or a planar lipid bilayer respectively. A summary of these analytical techniques have been reviewed elsewhere [3]. Overall, as transporters become more structurally and functionally diverse, there is also a need for need analytical techniques to evolve alongside to shed light on complex processes such as self-assembly, aggregation, and stimuli-response.

There has been tremendous progress in the field of synthetic ion transport in recent years, and the biological effects of ion transporters are beginning to be investigated. Transporters can activate cell signalling pathways such as apoptosis, and cause changes in biological micro-environments such as lysosomal pH, although there is still much to learn about the biological impact of different ion transport processes [4–6]. End applications include discovering agents that produce either a therapeutic effect by replacing the function of faulty biological channels, or a toxic effect that can arise by disrupting vital biological ion gradients in target cells [7,8]. Furthermore, ion transporters themselves are becoming more diverse, as a wider variety of supramolecular structures are being investigated. Recent advances have seen the development of stimuli-responsive ion transporters, whose activity can be controlled using triggers such as membrane potential [9–12], light [13–17], temperature [18], pH [19], reduction [20] and enzymes [21,22].

The majority of synthetic transport systems reported to date are based on purely organic scaffolds. However, there is increasing interest in the development of active ion transporters based on metal–ligand coordination constructs. The incorporation of charged metal ions into a necessarily lipophilic membrane transporter might seem initially counterintuitive – however, researchers have developed synthetic strategies to balance the solubility properties of their constructs to enable membrane partitioning and function. Coordination chemistry offers a versatile strategy to create diverse, highly tailored structures, as ligands can be modified to tune properties such as size, lipophilicity, flexibility, and function, whilst the metals provide different coordination geometries and a convenient attachment point for several functional groups. It is possible to introduce a variety of functional groups both pre- and post-assembly, and these can include groups to enable gating, lipid chains to promote membrane interaction, and reactive handles for bio-conjugation. The metal itself can also play a role in ion-binding, as coordination can have an electron-withdrawing effect, thereby polarising nearby groups for anion binding [23–25]. Additionally, certain metal ions can introduce desirable properties such as luminescence to the complexes formed. The solubility of metal–organic architectures can be readily tuned [26], and stimuli-responsive behaviour can be engineered [21,27] to produce additional useful function. Encouragingly, metal–organic constructs have already found application as therapeutics [28,29], diagnostics [30] and delivery vehicles [31,32], which paves the way for the further application of metal–organic transport systems as therapeutics.

In this article, we will review the development and application of metal–organic architectures as ion transport systems. We will highlight the advantages of incorporating metal–ligand coordination chemistry into the design of membrane transporters, alongside key design strategies that have emerged from existing work in this field, and the exciting potential for further advancement.

## 2. Ion channels and membrane-spanning constructs

Ions bear an electrostatic charge, and therefore they are often too hydrophilic to pass through biological membranes. In biology, ions commonly move through membrane-spanning protein channels which provide a pore through which ions can move. Depending on the size and shape of these pores, certain ions can be screened out selectively while others pass through (e.g., the potassium channel) [33]. Synthetic channels must therefore resemble natural channels in some aspects, and commonly, they have a membrane-spanning lipophilic domain. They can either have an intrinsic pore or self-assemble to form a pore through which ions can pass. Due to the requirement for large molecular structures to span membranes, self-assembly has been explored as a promising building strategy to large, complex structures, and metal coordination in particular can facilitate the self-assembly of ligands to create functional structures. In this section, the coordination-drive self-assembly of functional ion channels is reviewed based on the metal chosen to template the formation of the membrane-spanning structure.

### 2.1. Palladium

Palladium(II) is a popular metal ion of choice for building synthetic ion channels, as palladium-ligand bonds have highly predictable and rigid square planar coordination geometries, which allow for the predictable assembly of ligands into larger architectures. Thus, the coordination between palladium and hydrophobic ligands is often explored as the driving force for the self-assembly of small molecules into functional supramolecular ion transporters.

The earliest example of a membrane spanning Pd(II) complex was published by Fyles and Tong in 2007 [34]. The macrocyclic complex **1** was based on a structure initially reported by Ogura and co-workers [35] and was subsequently modified to bear lipophilic membrane-spanning anchors. The structure in Fig. 1a) builds upon a tetrameric square opening comprised of four 4,4-bipyridine ligands constructed via coordination to Pd(II) ions in each corner. Additionally, each square planar palladium corner is coordinated to a chelating ethylene diamine ligand appended to a C16 alkyl chain which was intended to span the length of the phospholipid membrane (Fig. 1b)). Interestingly, ion conductance experiments lead to the observation of three types of behaviour; initial erratic behaviour followed by occasional, short channel-like openings, followed by frequent very long-lived and highly conducting channel openings. These long-lived channels were presumed to involve an extended aggregate of the palladium complex and lipids surrounding a toroidal pore in the membrane. Ultimately, these results highlight that self-assembled systems may not be static, and that aggregation and dynamic structural interconversion are important factors that must be considered.

The work of Tong and co-workers [34] established that Pd(II) can play a structural role in assembling active ion channel components. Building on this concept, Wilson and Webb were able to use the dynamic assembly/disassembly of Pd(II) complexes to construct gated ion transporters [36]. In this system, the addition and removal of palladium was used to reversibly control the assembly of membrane-spanning channels based on ligand **L1**, a pyridyl cholate lipid (Fig. 2). In order to achieve palladium-gated

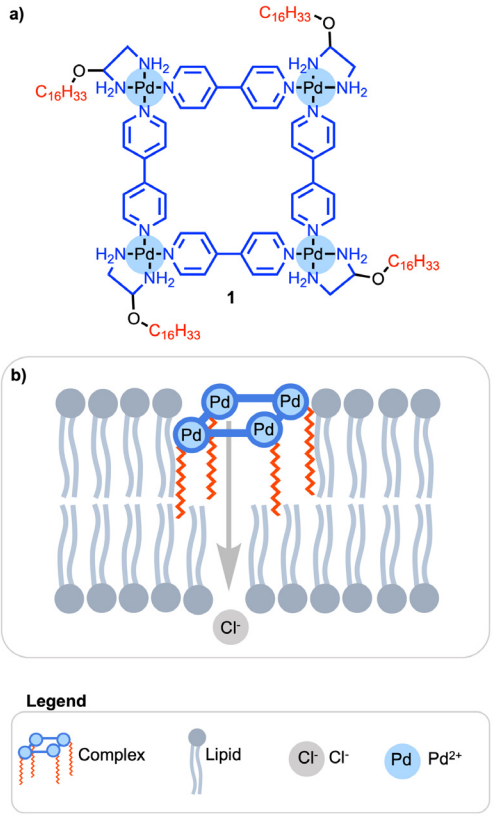


**Fig. 1. a)** The structure of a palladium-based tetrameric square complex with the coordinating moieties shown in blue and lipophilic membrane anchors shown in red. **b)** A representation of the intended membrane-spanning structure [34].

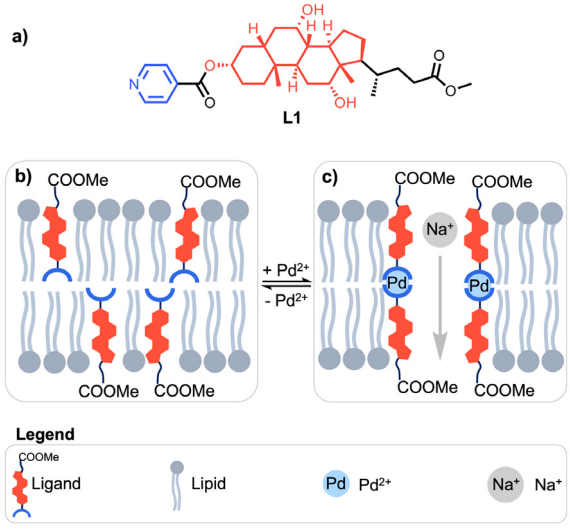


**Fig. 2. a)** The structure of pyridyl cholate-based ligands with the lipophilic moiety (red) and palladium-coordination site (blue). **b)** A representation of the inactive channel. **c)** A representation of the coordinated, active channel [36].

ion transport, the authors utilised the HPTS assay [37] (based on the pH responsive fluorescent probe 8-hydroxypyrene-1,3,6-trisulfonic acid) to assess sodium transport. They observed no ion transport using **L1** alone; however, upon addition of $PdCl_2$ to vesicles co-assembled with the ligand, ion transport was observed due to the formation of a membrane-spanning complex. Ion transport was also observed upon addition of the pre-formed Pd(II)-(**L1**)$_2$ complex to vesicles. Furthermore, the reversibility of the ion conductance was demonstrated after two rounds of palladium addition followed by palladium removal using the chelator, 18S6, which scavenged and removed the palladium from the assembly. Thus, the activity of the self-assembled channel could be controlled through dynamic assembly and disassembly, providing a route to bio-reminiscent gating behaviour.

To further explore novel mechanisms for the gating of channels, Webb and co-workers utilized binding interactions between channel components and biomolecules to control the spacing and geometry of ligand **L2**, which assembled to form Pd(II)-pyridyl cholate-based ion channels (Fig. 3) [38]. In a similar mechanism to the system reported by Wilson and Webb [36], the addition of palladium functions to cross link two pyridyl cholate ligands to yield a membrane-spanning structure capable of ion conductance (Fig. 2c) and 3c)). The ligands were also functionalized with biotin, which was designed to be presented on the membrane surface. Upon addition of multivalent avidin, a decrease in ion flow was observed via the HPTS assay and conductance measurements. This suggests that avidin was able to bind to the biotin moieties and block the channels or alter the spacing between the membrane spanning complexes to be non-ideal for transport. Additionally, aggregation of the biotin-bearing vesicles was observed, as binding to multivalent avidin binding can potentially bridge the membrane-spanning complexes on different vesicles (Fig. 3d)). Overall, this paper reflects the importance of spatially appropriate pre-organization when generating active supramolecular assemblies and the potential for biopolymers to regulate the activity of synthetic constructs.

While the spatial organization of channel components can be altered by external interactions, multi-metallic architectures can form a variety of interesting geometries. Therefore, coordination

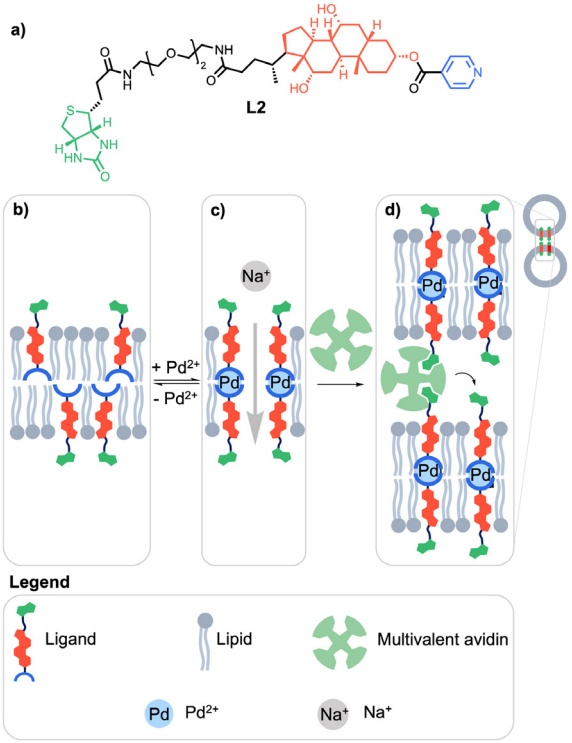


**Fig. 3. a)** structure of the biotin-appended pyridyl cholate ligand with the hydrophobic moiety (red), Pd(II) coordination site (blue) and avidin binding site (green); **b)** a representation of the inactive channel, and **c)** a representation of the coordinated, active channel. **d)** A representation of disrupted channel arrangement and vesicle aggregation caused by multivalent avidin binding [38].

to metals can instigate the arrangement of large, planar ligands into active, 3-dimensional, porous structures. This strategy was explored in 2011 by Webb and co-workers, wherein membrane spanning bis(*meso*-3-pyridyl) porphyrin ligands (**L3**) oligomerized to form pores upon the addition of Pd(II) in solution and in the lipid bilayer membrane (Fig. 4a)) [39]. A trimeric cyclic structure was proposed to be the active species, forming a triangular pore with the porphyrins constituting the faces of the structure whilst Pd (II) ions connected the edges (**2**, Fig. 4b)). However, in solution phase studies, linear oligomers appeared at higher concentrations, and the identity of the trimeric pore was inferred at concentrations below 2 mM. The membrane-active species was shown to transport anionic 5/6-carboxyfluorescein. The authors proposed that this dye could be transported through the triangular openings of the trimeric pore.

Metal coordination complexes have the potential to assemble into aggregated porous structures, and in some cases, these aggregated metal complexes have been investigated as long-lived stable pores. Similarly, inherently porous metal–organic assemblies may form ion conducting channels, and this strategy was investigated by Kempf and Schmitzer in 2017 [40]. In this report, two types of transporters were developed based on the Pd(II) mediated self-assembly of functionalized 2,4,7-triphenylbenzimidazole ligands (Fig. 5). Although the structure of the active species is unknown, computational modelling suggests that individual Pd(II)-$L_2$ complexes were found to further associate either via pi-stacking interactions for complex **3**, or direct coordination for complex **4** to form a porous aggregate. For complex **3**, it was proposed that 4 units were required to span the length of the lipid bilayer, whilst for complex **4**, 3 units were required. This aggregation behaviour is supported by gel formation in DMSO. While conducting studies on the antibacterial properties of these metal–organic assemblies, the authors found that complex **4** had a minimum inhibitory concentration (MIC) of approximately 40 μM against *B.* thuringiensis. However, addition of $PdCl_2$ to *B.* thuringiensis-incubated complex **4** (1 h) reduced the MIC value to approximately 20 μM, indicating the ability of Pd(**4**) to alter bacterial membrane permeability. The permeability of these assemblies was tested in a *B.* thuringiensis tetracycline-resistant strain. Here, the authors found that both **4** and Pd(**4**) decreased the tolerance of the bacteria to tetracycline, but that Pd(**4**) was more effective. Overall, chloride transport was observed, and the treatment of bacterial membranes with the transporter increased their permeability to antibiotics.

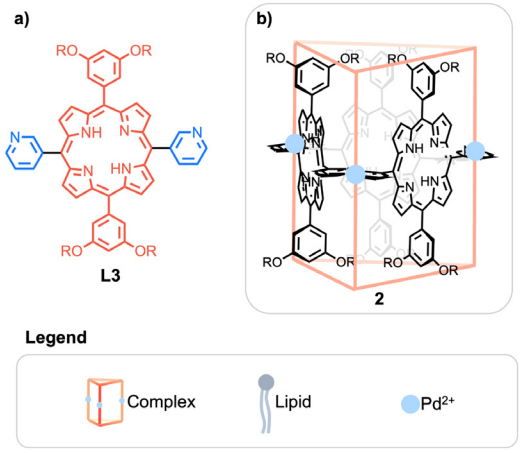


**Fig. 4. a)** The structure of ligand **L3** reported by Webb and co-workers [39]; **b)** the proposed structure of the active trimeric pore, through which anionic dye molecules could be transported.

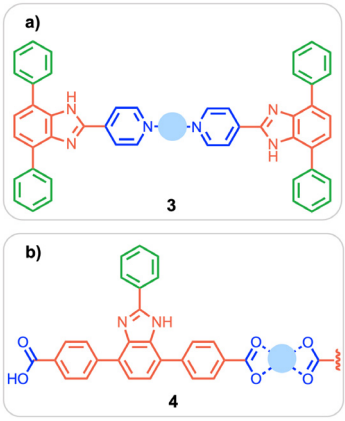


**Fig. 5. a)** The structure of complex **3** reported to assemble into membrane-spanning channels by Schmitzer and co-workers [40]. **b)** The structure of complex **4** reported by the same authors. Colour scheme: hydrophobic parts (red), pi-stacking benzyl groups (green) and coordinating ligands to palladium (blue).

### 2.2. Copper

Copper-ligand complexes also have several advantages for use in constructing ion transport systems. Copper complexes are highly stable in biological contexts [41], and, in small concentrations, copper ions have a low toxicity in the body [42]. Although copper paddlewheels are sensitive to water [43], inside the lipid bilayer, they have proven to be useful scaffolds in the design of metal–organic architectures. One example of its use as an ion transporter is given in the section below.

The first example of a copper-based ion channel was published by Matile and co-workers in 1999 [44]. The authors designed the channel with a ligand (**L4**) containing two main functionalities – a Cu(II) ion binding site, and a rod-shaped pi-slide (Fig. 6a)). The ligand-binding site consisted of an iminodiacetate (IDA) group, which allowed for ligand aggregation, and subsequent channel formation through polyhistidine (pHis) binding to copper (II) ions (Fig. 6b) and 6c)). This aggregation in turn created a cation binding site between two rod-shaped pi-slides, and potassium transport was confirmed *via* the HPTS assay. Matile and co-workers found that it was possible to block channel activity with tetraethylammonium (TEA) cations – hypothesising that this large cation binds to the pi-slides.

Kim and co-workers published another example of a copper-based ion channel (complex **5,** Fig. 7) in 2008 [45]. The channel itself was based on a metal–organic polyhedron MOP-18, with a large internal cavity studied extensively by Yaghi and co-workers (Fig. 7a)) [46,47]. In this work, Kim and co-workers introduced a hydrophobic shell to allow for facile insertion into bilayers. Using an HPTS assay, this channel was determined to transport protons and alkali metal ions, as shown in Fig. 7c). Here, the Cu(II)-paddlewheels (Fig. 7b)) play a structural role in the construction of the polyhedron that defines the cavity of the channel.

Another example of the use of copper within ion channel formation was reported by Gokel and co-workers in 2009 [48], shown in Fig. 8 – the authors synthesised nanocapsules appended with hydrophobic chains, one capsule which assembled *via* the coordination of Cu(II) ions to ligand **L5** (complex **6**), and a similar capsule which assembled *via* hydrogen bonding interactions. Using planar bilayer conductance (PBC) measurements, the authors determined that channel-like behaviour was only observed in the copper-seamed capsules. This implies that the copper played a structural role, which in turn, allows for the channel-like properties of these molecules.

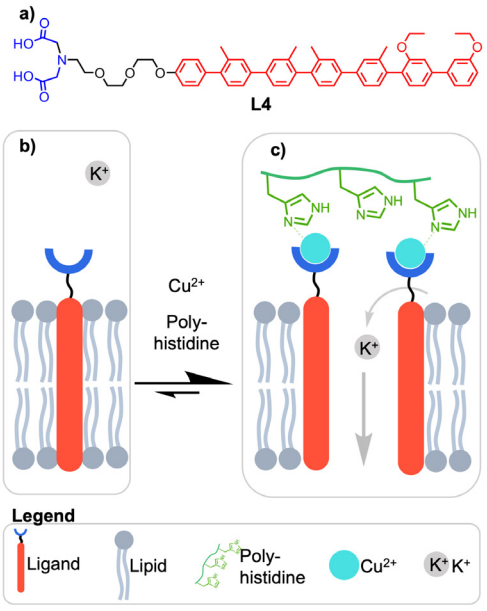


**Fig. 6. a)** Copper-based ion channels have a hydrophobic pi slide (red), and a copper-coordinating iminodiacetate head group (blue) [44]. **b)** The ligand is able to insert into the membrane, and **c)** aggregation caused by polyhistidine binding is proposed to bring the ligands into close proximity to form a channel.

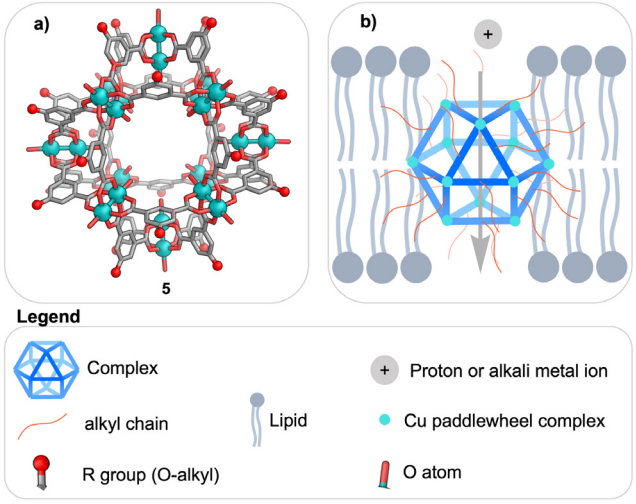


**Fig. 7. a)** The crystal structure of MOP-18-based metal–organic polyhedron [46,47]. **b)** The copper paddlewheel structural motif. **c)** The functionalisation of MOP-18 with hydrophobic alkyl chains yielded complex **5**, which can partition into a membrane and enable ion transport through the porous structure [45].

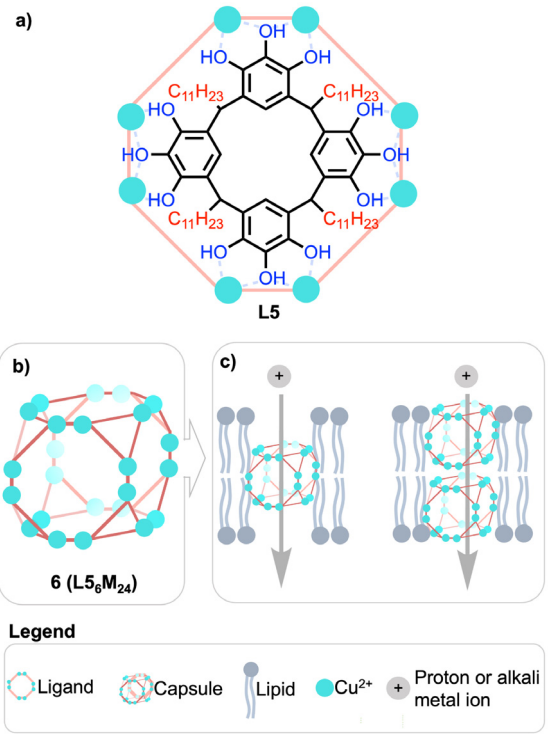


**Fig. 8. a)** Pyrogallol ligands **L5** contain copper binding sites (dark blue) and hydrophobic alkyl chains (red). **b)** Six ligands are proposed to self-assemble to create a copper-seamed capsule **6**, and **c)** these porous capsules are thought to insert into the membrane and enable the transport of protons or group 1 metal ions – two proposed channel formation mechanisms are shown, involving ion passage through either one or two capsules [48].

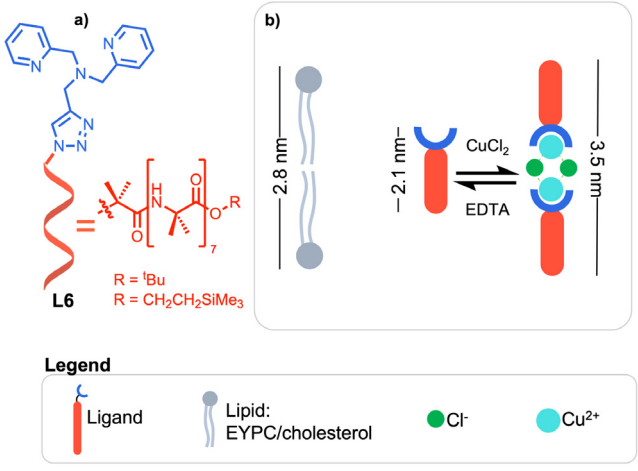


**Fig. 9. a)** The structure of ligand **L6** consisting of a copper-binding moiety (blue) and a membrane-spanning hydrophobic coiled foldamer (red). **b)** The dimensions of all components – lipids, unbound ligand and bound metal–ligand complex [49].

In 2020, Webb and co-workers reported the synthesis of a switchable ion channel [49]. Much like the example reported by Matile [44], metal-coordination was used as a tool to drive the assembly of multiple membrane-spanning units (**L6**) to 'switch on' ionic conductance. In this case, the channel was composed of a chloro-bridged copper dimer complex. Each ligand consisted of a metal chelating unit and a large hydrophobic foldamer (Fig. 9a)). One foldamer was not able to interact with and span the phospholipid membrane. However, upon the addition of $CuCl_2$ to the membrane, two ligands were able to aggregate and bind the copper(II) ions, which formed the active species. The removal of copper(II) ions via addition of EDTA was subsequently used to 'switch off' channel activity (Fig. 9b) and 9c)). Low cation selectivity was shown via the HPTS assay, while greater anion selectivity was observed, and the transport of chloride was confirmed via assays using the halide sensitive dye lucigenin. Channel-like behaviour was confirmed via PBC measurements. The authors then measured the antibiotic activity of **L6** (where R = $^t$Bu and $CH_2CH_2SiMe_3$) against a strain of *B.* megaterium bacteria. The MIC of the Cu-**L6** complexes were significantly lower than **L6** only. In fact, these complexes show similar activity to alamethicin, a channel-forming peptide antibiotic; however, these complexes

are not suitable for use in clinic due to their low haemolytic activity.

Another example of a copper(II) gated system was reported in 2021 by Ohba and co-workers. In this example, amphotericin B served as the membrane-spanning unit which was functionalised with bipyridine to bind Copper(II). The complex displayed pH-dependent and Cu(II) gated permeability to $Ca^{2+}$, which was assessed via the use of POPC vesicles loaded with Asenazo III, a colourimetric indicator for calcium [50]. When Cu(II) is present at pH 9, a dinuclear $Cu(II)_2(\mu\text{-}OH)_2(\mathbf{L7})_2$ complex is proposed to provide parallel orientation of two ligands with a distance of about 8 Å as suggested by the crystal structure (Fig. 10). Aggregation of the ligand in POPC liposomes is suggested due to the observed hypsochromic shift in the heptaene absorbance, whilst circular dichroism revealed a weakly absorbing couplet when copper was added at pH 9.0, suggesting channel assembly via parallel association of the amphotericin moiety.

### 2.3. Zinc

Zinc(II) is another popular choice of metal ion for the construction of metal–organic cages and frameworks. Zinc ions are also essential for various biological processes, like growth, reproduction, and immune function. This may be advantageous for use in biological contexts due to the low toxicity of the component metal ions.

Kobuke and co-workers [51] designed a molecular nanopore composed of self-assembled zinc porphyrin-based macrocycles with the aim of synthesising a structure that resembles photosynthetic light-harvesting antenna. Three zinc porphyrin-containing units (**7**, Fig. 11a) self-assembled to create a macrocycle ($\mathbf{7}_3$) which was cross linked via metathesis (Fig. 11b)), and the authors propose that two macrocycles interact to span the bilayer (Fig. 11c)).

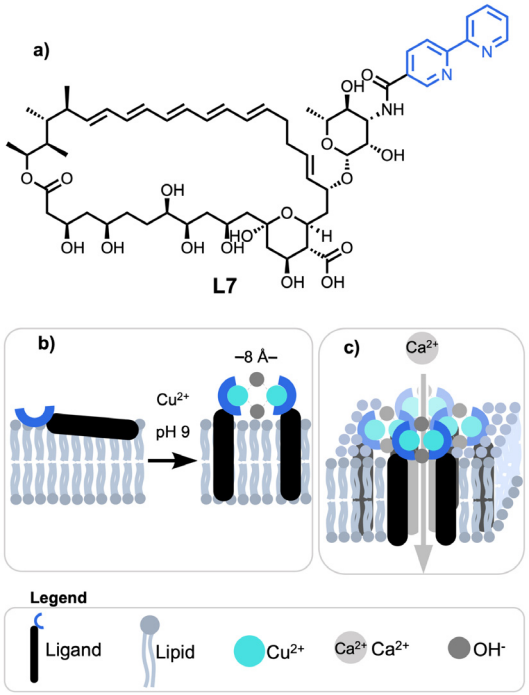


**Fig. 10. a)** Structure of an amphotericin B-bi-pyridine conjugate **b)** Schematic representation of **L7** interacting with the lipid membrane before and after Copper (II) complexation at pH 9. This leads to the formation of hydroxide bridged dinuclear complexes. **c)** The dimerised complex is proposed to aggregate to form pores [50].

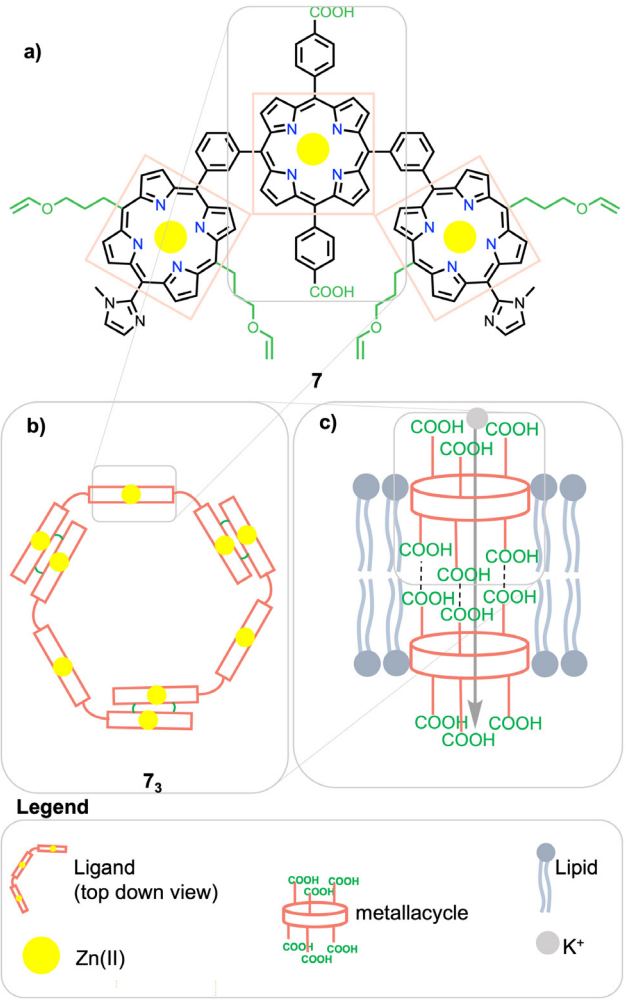


**Fig. 11. a)** A zincated porphyrin-based structure **7** reported by Kobuke [51] **b)** Three ligands can self-assemble to create a metallocycle, which is subsequently cross-linked through alkene metathesis and **c)** two cross-linked metallocycles are thought to self-assemble to span the membrane.

In this case, the Zn(II) porphyrins provide a rigid skeleton upon which large, stable macrocycles can be built. Here, the macrocycles contain six carboxylate groups that point up and down to aid with insertion into, and interactions with, the hydrophilic part of the lipid bilayer membrane – using PBC experiments, these groups were found to be crucial for channel activity, as analogues without carboxylate groups were shown to be inactive. The carboxylate ions also play a role in switching the channel on and off. The authors found that electrostatic interactions with cationic amino groups on poly(amidoamine) (PAMAM) dendrimers block the channel opening, and when removed, the channel turns on again. Generally, such large pores are unlikely to show any selectivity – Kobuke and co-workers showed that even large tetrabutylammonium cations can pass through. In the presence of TMACl, the authors observed a moderate cation selectivity.

In 2017, Haynes, Keyser and Nitschke [52] reported the ion channel activity of a $Zn_{10}(\mathbf{L8})_{15}$ prismatic assembly **8** (Fig. 12a–b)). The active channel species (**8**) was formed via subcomponent self-assembly – a technique that utilises amines and aldehydes, as well as a metal-ion template, to synthesise imine-based metal–organic architectures. Due to its unique structure the pentagonal prismatic complex can bind three types of anions in distinct pockets – perchlorate anions bind within peripheral binding

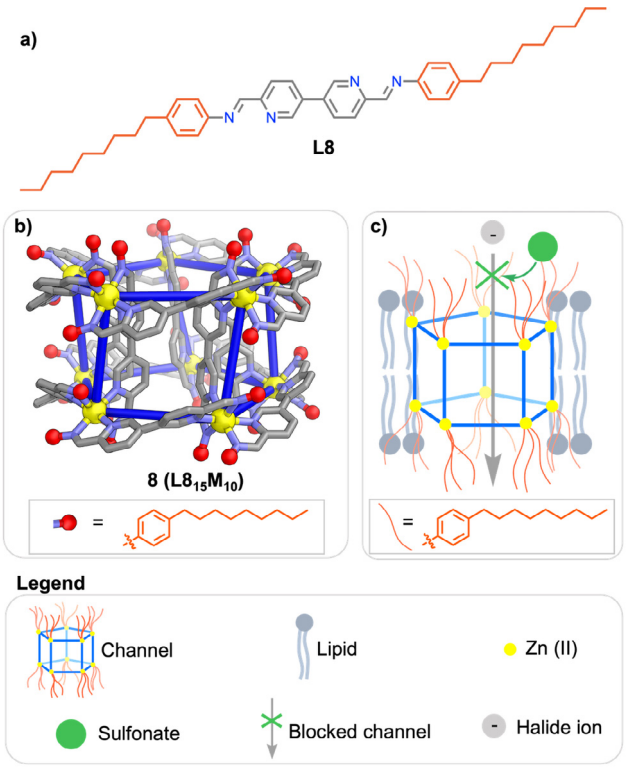


**Fig. 12.** a) The structure of ligand **L8** bearing sites for metal coordination (blue) and lipophilic alkyl chains (red), which can self-assemble into a pentagonal prismatic complex [52] **b)** A crystal structure of the complex composed of 15 ligands (grey), and 10 zinc ions. The position of the lipophilic chain in complex **8** is shown in red. **c)** A schematic representation of the complex interacting with the lipid bilayer aided by the lipophilic chains.

pockets, halide ions bind within the toroidal pore of the prism, and sulfonate ions bind above and below the prism. The initial observation of halide ion transport led to investigation into larger anions being transported through the central cavity, however, only selectivity for halides was seen. The transport was not observed to be cation dependent. Given the finding that that sulfonate ions could bind above and below the pore, the authors hypothesised that sulfonate ions could be used to block channel activity (Fig. 12c)). Correspondingly, they found that the addition of sodium dodecyl sulfate (SDS) could effectively block the ion channel.

It is possible to achieve precise spatial organisation of ligands *via* metal–ligand coordination, and in a recent publication, Liu and co-workers synthesised three $Zn_4L_4$ metallocycles **9** with functionalised sub-nanometre apertures (Fig. 13) [53]. 1,1′-bi-2-naphthol-based ligands were functionalised with hydroxyl, ethoxyl, and pentaethylene glycol groups facing towards the centre of the pore. UV–vis titrations were used to determine the binding constants of the 3 complexes towards halides, and all complexes displayed the trend $I^-$>$Br^-$>$Cl^-$ from strongest to weakest binding respectively. The HPTS assay was used to assess halide transport and revealed that the ethoxyl substituted metallocycle displayed selectivity of up to 38x for $I^-$ compared to other halides ($Cl^-$ and $Br^-$) in line with the Hofmeister series, whilst the pentaethylene glycol substituted complex showed little selectivity, but had a lower $EC_{50}$. The HPTS assay conducted with different cations revealed that transport is not cation dependent whilst an assay using the halide responsive dye lucigenin confirmed that the channel itself can mediate $Cl^-/NO_3^-$ antiport. Channel-like behaviour was confirmed via patch clamp measurements.

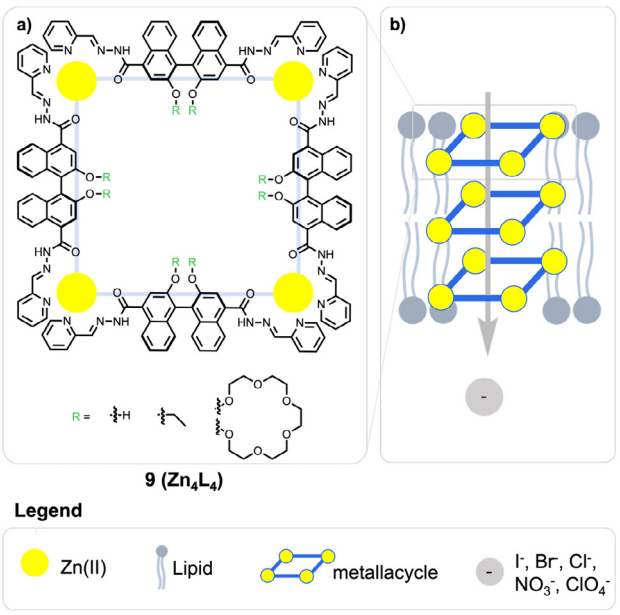


**Fig. 13. a)** 1,1′-bi-2-naphthol-based ligands were functionalised with hydroxyl, ethoxyl, and pentaethylene glycol groups, and were incorporated into $Zn_4L_4$ metallocycles **9**. **b)** It was proposed that the metallocycles could pack to form a nanotube and thus a pathway for ionic conductance through a lipid bilayer [53].

### 2.4. Other metals

Ongoing research is seeking to expand the toolbox of metal complexes that can be applied in the design of functional ion transporters. Diversifying the metal building-blocks used enables access to a wider variety of geometries that can be applied to build increasingly complex structures such as catenanes, capsules and polyhedra, whilst polyvalent metal–ligand bonds provide an anchoring point for a variety of functional moieties such a lipophilic chain, and structural motifs. Furthermore, metal–ligand bonds can have varying stabilities and reactivities, and this can be used to achieve reaction-based control of essential properties such as self-assembly, valency and conformation. Lastly, the inclusion of metals into structures such as porphyrins, can greatly change the physical properties of the transporter such as lipophilicity, solubility, and charge, and these are essential in tuning the activity and function of ion transporters.

Inspired by Kobuke and co-workers [51], Tecilla and co-workers reported a zinc porphyrin-based nanopore in 2012 [54]. The authors chose to incorporate the zinc into the porphyrin ligands (**L9**, Fig. 14a)) to improve the solubility of the overall channel. Meanwhile, the metallocycle **10** was assembled via interactions between pyridyl donors and Re(I) ions (Fig. 14b)). The authors incorporated carboxylate groups into the scaffold to enable interactions with the hydrophilic portion of the lipid membrane, to mediate metallocycle stacking and to allow for on/off activity through electrostatic interactions with amino groups on PAMAM dendrimers, as previously shown by Kobuke [48]. Channel activity was inferred via a HPTS assay in 100 nm liposomes.

In 2014, Winterhalter and co-workers synthesised an amphiphilic cobalt-based structure capable of pore formation (**11,** Fig. 15a)) [55]. The Co(III) ion plays a crucial role in formation of the positively-charged amphiphile headgroup, and the interaction of the complex with negatively-charged phospholipid head groups allows for high biological activity within lipid bilayers. The ‘tail’ portion of the amphiphile is composed of a long alkyl chain, containing a crown ether moiety able to coordinate cations and aid ion transport. The authors proposed pore formation occurring via

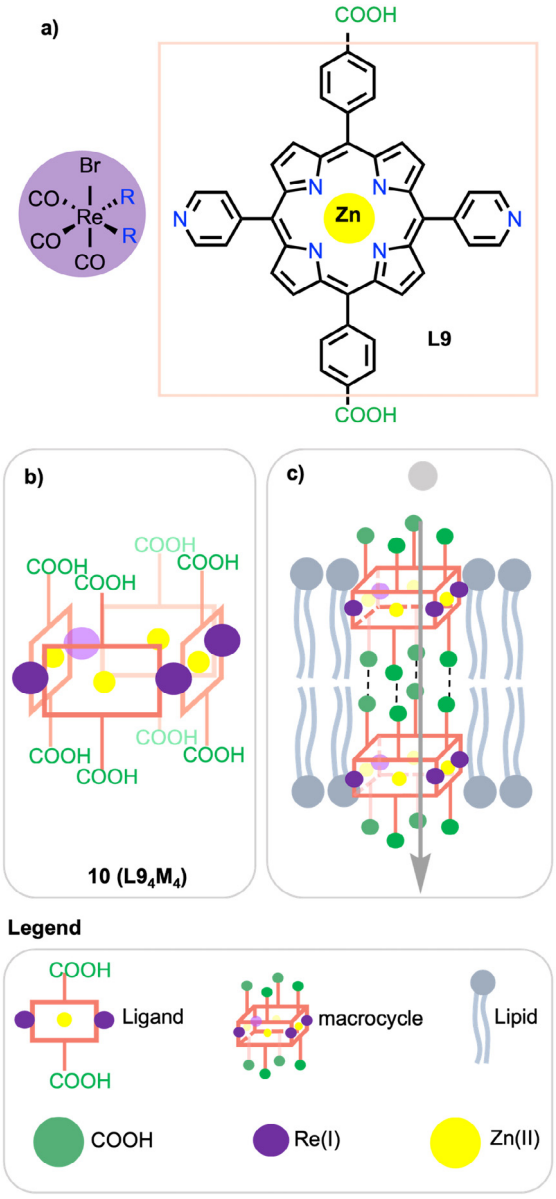


**Fig. 14. a)** A zincated porphyrin ligand **L9** containing two pyridyl units for coordination to a Re(I)-based metal complex [54]. **b)** The complexation is thought to form square metallocycles consisting of four ligands held by Re(I)-based corners. **c)** Two metallocycles are thought to interact to span the bilayer.

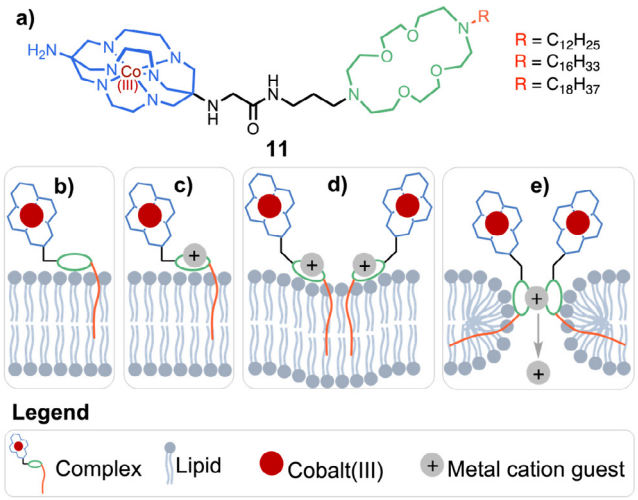


**Fig. 15. a)** Amphiphilic ligand **11** is composed of a cationic cobalt head group (blue) and a lipophilic tail composed of crown ether cation binding group (green) and a lipophilic chain (red) [55]. The authors propose that **b)** the lipid inserts into the membrane, **c)** binds a cation, and **d-e)** can dimerise to cause membrane curvature and the formation of pores.

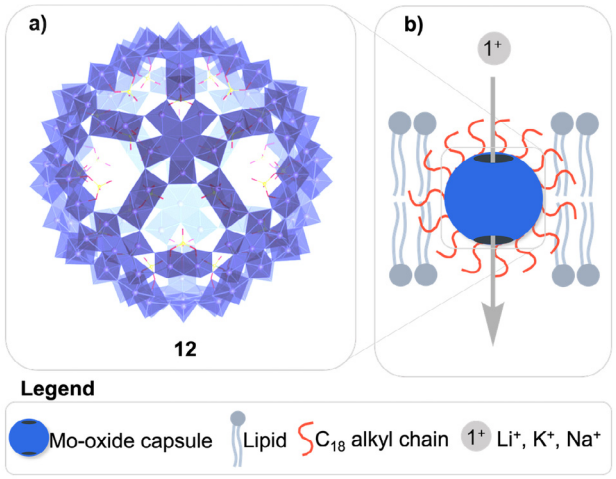


**Fig. 16. a)** A representation of a molybdenum oxide capsule **12**, which was subsequently modified to bear alkyl chains *via* surfactant attachment [56]. **b)** The alkyl chains promote interaction with the membrane whilst cations can move through the porous capsule.

two amphiphile units coming together and inducing curvature within the bilayer leaflet – this curvature strain causes ion pore formation and eventual cell rupture (Fig. 15 b–e)).

Barboiu and co-workers reported porous, molybdenum-based metal-oxide capsules that could function as ion channels in 2015 (Fig. 16a)) [56]. The capsules (**12**) were surface-functionalised with an organic surfactant to enhance their lipophilicity and allow for incorporation into the lipid bilayer (Fig. 16b)). The capsule was formed of different molybdenum units, all with different oxidation states – but ultimately, the role of the metal was, once again, structural. Using HPTS assays, the authors found that the channel can mediate cation transport and does show some cation selectivity within the alkali metals, depending on the desolvation rates of the cation.

As shown by Kim and co-workers (2008) [45], the cuboctahedral geometry is useful for synthesising synthetic ion channels – its unique geometry provides cavities and apertures for ion to pass through. Furukawa and co-workers utilised complex **13**, a cuboctahedral Rh(I) metal–organic polyhedron (MOP), as an ion channel in 2017 [57]. The authors incorporated long alkyl chains into the MOP scaffold to facilitate incorporation into the lipid bilayer – however, interestingly they found that the length of the chain was proportional to the opening time of the channel. They reasoned that the MOP structure can rotate within the lipid bilayer, with ionic conductance occurring through either the triangular or square apertures, and hence shorter chains allowed for faster rotation and thus a shorter channel opening time (Fig. 17a), and 17b)).

Li and co-workers used Cd(II) ions to direct the formation of discrete, nested, hexagonal structures called Kandinsky circles [58]. The corners of the Kandinsky circles were comprised of bent, multi-layered bis-terpyridine ligands **L10** (Fig. 18a). Depending on the degree of cross-linking in the ligand, a range of structures of increasing diameter comprised of 1–4 nested hexagons were produced (Fig. 18b) and 18c)). Through PBC measurements, the authors found that the complexes containing 2, 3, or 4 nested

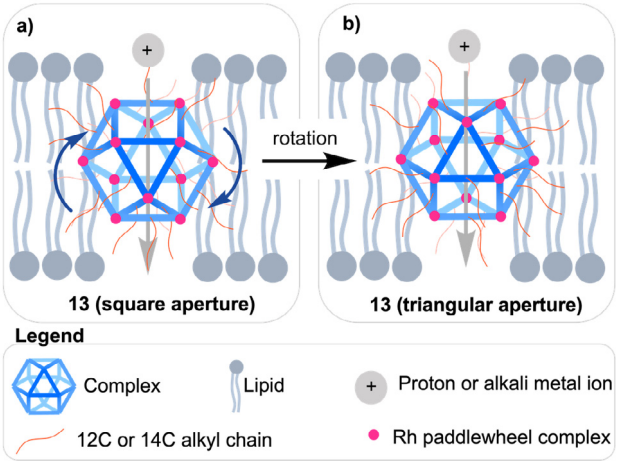


**Fig. 17. a)** The cuboctahedral complex **13** can transport cations through either square apertures or **b)** triangular apertures, and rotation of the complex causes switching between the two pathways [57].

hexagons could incorporate into lipid bilayers to form a web-like structure, able to form a transmembrane channel within bacteria-like lipid membranes (Fig. 18d)). This in turn imparted antimicrobial effects against MRSA. Patch clamp analysis in KCl showed stepwise conductivity, confirming ion transport via a channel.

Although not as common, iron compounds have been reported in the construction of ion transporters. One such example was published recently by Hamada and co-workers [59], in which modified Prussian blue nanoparticles (PB NPs **15**) were investigated as ion transporters and were found to be good ionic conductors in liposomal membranes (Fig. 19a)). To increase the hydrophobicity of the nanoparticle, the authors modified the surface of the PB NPs with hydrophobic oleyamines (Fig. 19b)). In these nanoparticles, the role of the metal ions varies – they provide structural support to the nanoparticle, while aiding with ionic conductivity too. The authors found that, *via* HPTS assays, it is possible to transport hydroxide ions across the lipid membrane using PB NPs.

Leigh and co-workers have also exploited the coordination chemistry of Fe(II) in the construction of synthetic ion transporters [60] as they explored use of interlocked structures including an $(Fe^{II})_5$ pentafoil knot, an $(Fe^{II})_6$- Star of David (Fig. 20a)) and a metal-free Star of David catenane – as ion channels. These structures each contain a central cavity, which could serve as a binding site and passage for ion conductance. The authors found that the metallated Star of David structure **16** could function as an anion channel (Fig. 20b)), while the smaller $(Fe^{II})_5$ structure showed reduced activity, showing that the size of the architecture can play a role in determining transport efficiency. Interestingly, two structural analogues of the active $(Fe^{II})_6$ species – a de-metallated Star of David [2]Catenane and a closely related $(Fe^{II})_6$ cyclic helicate – showed no transport activity (Fig. 20c) and d)), showing that both the presence of the metal and the final ring closing step is vital for ion transport to occur (Fig. 20c) and 20d)).

While metal ions can impart structural stability and direct assembly, it is also important to consider the functionality of the ligands. In a recent example published by Liu and co-workers, six chiral BINOL-derived ligands were used as spacers between four *n*-$Bu_3$-$Cp_3Zr_3$ clusters as vertices to yield a tetrahedral cage assembly (Fig. 21a) and b)) [61]. The intrinsically chiral cavity was decorated with a range of binding sites such as phenol, phenol-ether, and crown ether groups (R groups, Fig. 21c). This chiral cavity decorated with multiple binding sites allowed for the *enantio*-specific recognition of amino acids, as confirmed by fluorescence titrations

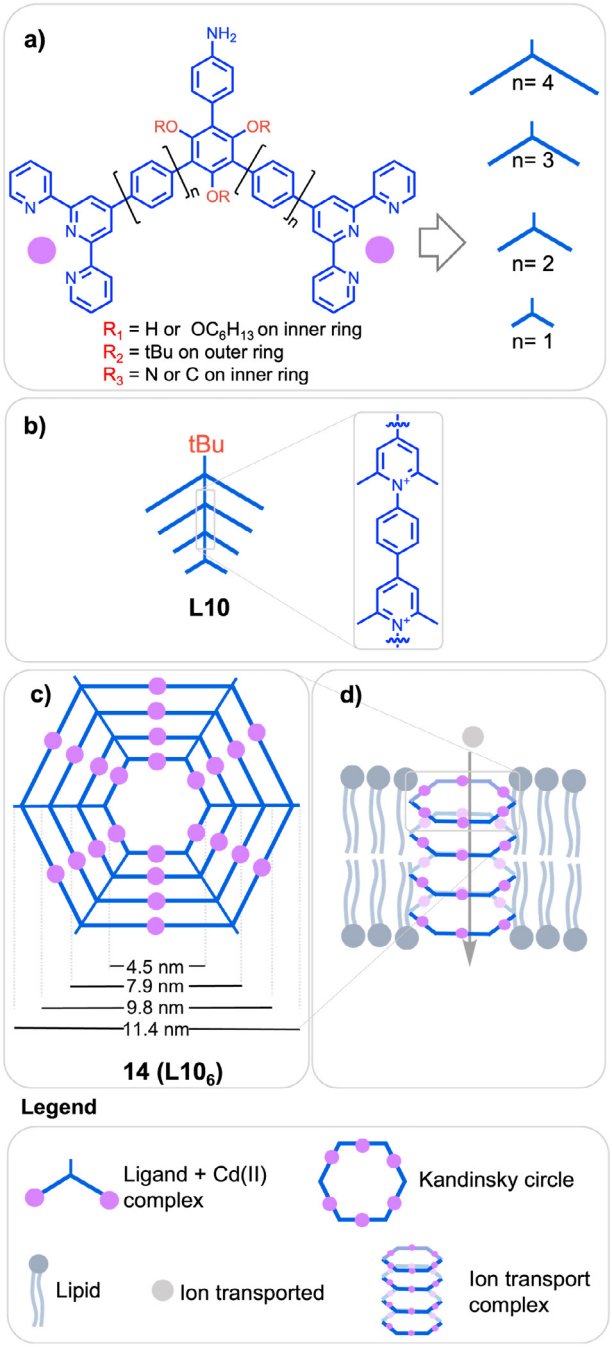


**Fig. 18. a)** The general structure of ligands **L10**. Ligands are increasing in size and can be cross-linked in a nested arrangement. The smallest inner-most ligand is appended with short alkyl chains (R1) and is cross-linked to larger ligands via pyridinium groups (*R*3), and the largest outer-most ligand is capped with a *tert*-butyl group (R2). **b)** Nested ligands can contain 1–4 units of increasing size crosslinked together. **c)** These ligands give rise to self-assembled Kandinsky circles of different sizes in combination with Cd(II) ions. In each case, the inner pore is 4.5 nm, whereas the outer diameter for structures containing 2, 3, and 4 nested units are 7.9 nm, 9.8 nm, and 11.4 nm respectively. **d)** Kandinsky circles containing 2–4 nested units are proposed to self-assemble into tubes that span the membrane [58].

with labelled amino acids. These cages were able to insert into lipid bilayers and the cage decorated with hydroxyl groups preferentially transported L-asparagine over D-asparagine, whilst the cage decorated with crown ether groups showed a preference for D-arginine over L-arginine (Fig. 21c). The cages were successfully

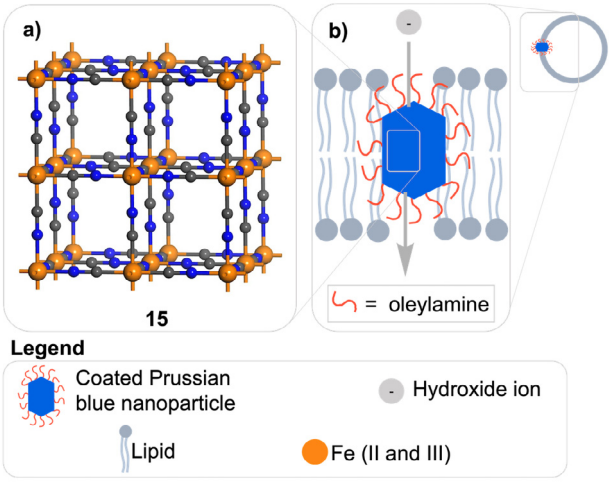


**Fig. 19. a)** The crystal structure of Prussian Blue. **b)** Prussian Blue nanoparticles were modified with a lipophilic coating to allow interaction with the lipid bilayer, and subsequent ion transport [59].

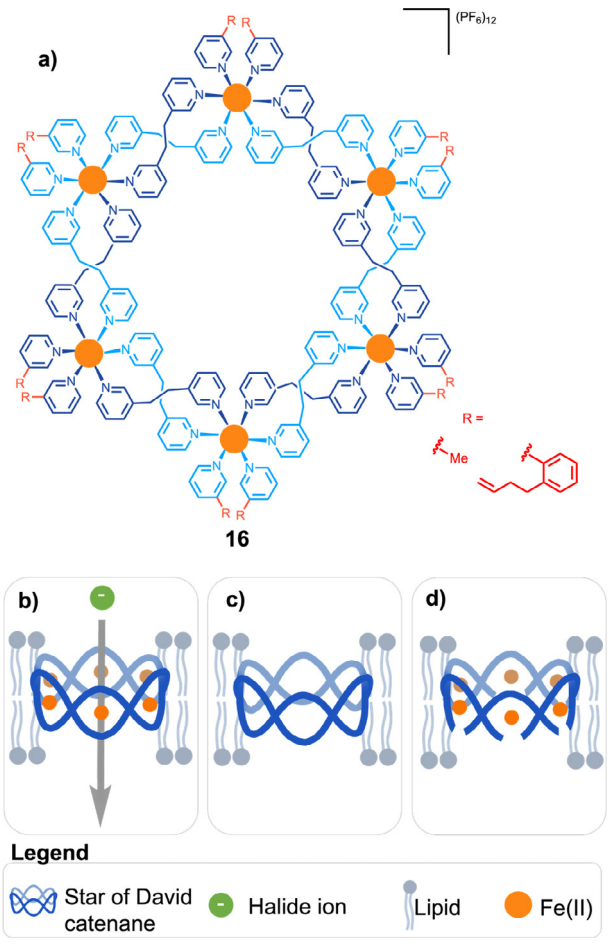


**Fig. 20.** a) The structure of the $(Fe^{II})_6$- Star of David catenane **16**, composed of pyridyl containing ligands (blue) complexed to Fe(II) ions (orange). **b)** The catenane complex transported halide ions. **c)** The de-metalated complex and d) the ring-open complex were unable to transport ions [60].

incorporated into the bilayer without causing lysis, as shown via a carboxyfluorescein dye release assay. Enantioselective amino acid transport was confirmed via dye-release assays via diffusion of

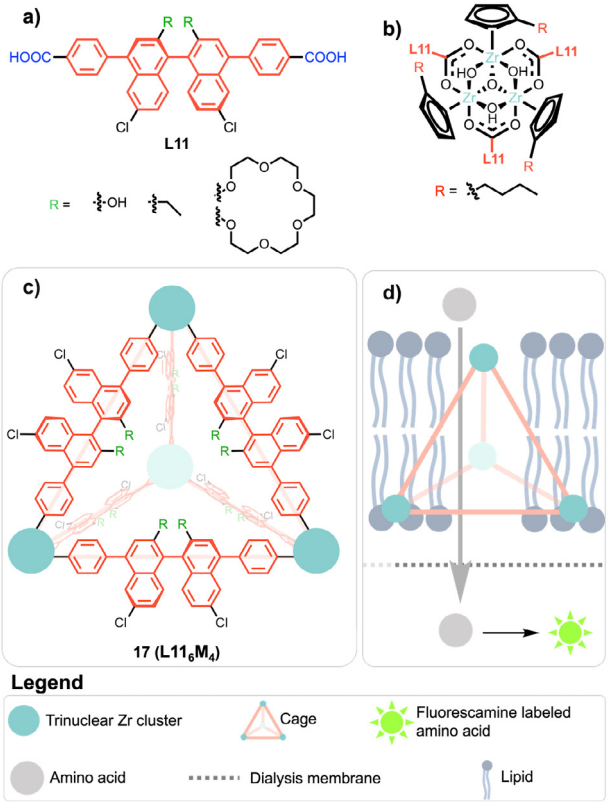


**Fig. 21. a)** chiral BINOL-based ligands **L11** were coordinated to $Bu_3$-$Cp_3Zr_3$ clusters. **b)** The overall triangular prismatic complex **17** contained a chiral cavity. **c)** Structure of the trinuclear Zr cluster. d) Amino acid release assays coupled with subsequent fluorescamine-labelling showed enantioselective transport [61].

transported amino acids through a dialysis membrane and subsequent labelling with fluorescamine (Fig. 21d).

## 3. Ion carriers

Ion carriers (also known as ionophores) offer an alternative strategy for ion transport across biological lipid membranes. While channels form a membrane spanning structure which allows ions to cross the bilayer, carriers can bind individual ions and provide a hydrophobic coating which allows them to passively diffuse into the phospholipid bilayer. Thus, carriers often have 2 structural components; ion binding sites, and hydrophobic moieties that enable effective membrane partitioning. All the carriers discussed here are anion transporters which bind either via metal–anion coordination and/or N—H—anion hydrogen bonding interactions.

A 2014 study by Tecilla and co-workers demonstrates the importance of having both an ion binding site and a hydrophobic moiety for ionophoric activity [62]. The ionophores **18** and **19** (Fig. 22) were built upon a square planar palladium complex bearing hydrophobic 1,3-Bis(diphenylphosphino)propane (dppp) ligands, which were inert to ligand exchange. The anion binding was achieved via the incorporation of exchangeable ligands ($OTf^-$ or $Cl^-$) which can be displaced by a guest anion. Interestingly, ionophore complex **18** demonstrated cation-independent and anion-dependent $OH^-/X^-$ antiport *via* the HPTS assay. The hydrophobic dppp ligand or $PdCl_2$ alone did not demonstrate activity, confirming that both the lipophilic ligand and the ion-binding site was necessary for activity. Furthermore, **18** bearing the more labile $OTf^-$ ligands was more effective at promoting pH-gradient collapse compared to **19** bearing $Cl^-$ ligands. Further anion transport activ-

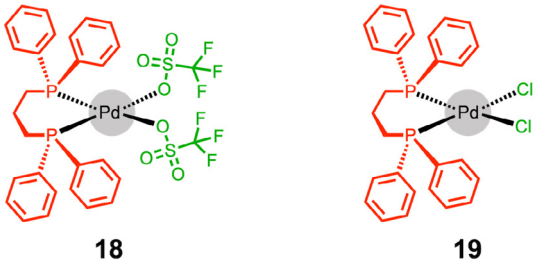


**Fig. 22.** Square planar anion carriers **18** and **19** comprised of a hydrophobic ligand (red) and an anion binding site revealed *via* exchange of labile ligands (green) [62].

ity was confirmed by a lucigenin fluorescence quenching assay. The proposed transport mechanism involves the monomer at low concentrations, or a bridged μ-OH- dimer at high concentrations, and binding occurs via halide exchange with $OH^-$. This mechanism is supported by U-tube experiments which demonstrates that **18** can transport Cl- across a bulk chloroform membrane.

Metal coordination has the potential to play a multi-faceted role, as a structural component which connects hydrophobic and guest binding sites, and as an optical label, as many metal complexes are emissive (such as those based on Ir, Re, Ru, and Eu just to name a few). Thus, the emissive properties of certain metal complexes allow them to be visualised in biological systems.

One such fluorescent anion carrier published in 2019 by Mao and co-workers reports an octahedral cyclometalated iridium complex bearing hydrophobic 2-phenylpyridine ligands, and an imidazole-based anion binding site [5]. Complexes **20** and **21** differ based on the presence of either 1 or 2 imidazole N—H binding sites respectively (Fig. 23). Cation independent $Cl^-/HCO_3^-$ and $Cl^-/NO_3^-$ antiport was observed via chloride selective electrode studies, and **20** was more active than **21**. The transport activity greatly increased when the pH outside the vesicles was raised from 4 to 7.2, demonstrating that deprotonation can have a profound effect on activity, and both complexes were determined to be carriers rather than channels as their activity decreased in vesicles containing cholesterol. Due to their potent $Cl^-$ transport activity, further biological studies were carried out, and treatment with the complexes led to cellular chloride influx, which was observed via the quenching of a chloride-sensitive fluorescent indicator N-(ethoxy carbonylmethyl)-6-methoxyquinolinium bromide (MQAE). The complexes were cytotoxic against a range of cancer cell lines, and the activity was found to be caused by reactive oxygen species (ROS) induced apoptosis. Furthermore, the weakly basic complexes accumulated in the lysosomes *via* the ion trapping effect, and the $Cl^-/HCO_3^-$ antiport activity was shown to raise lysosomal pH in cells, leading to lysosome dysfunction. This rise in lysosomal pH subsequently blocked autophagic pathways by inactivating hydrolases, and the presence of resulting autophagosomes with undigested cellular components was observed using transmission electron microscopy. Ultimately, both complexes also demonstrated *in vivo* anticancer activity as they inhibited tumour growth in mice, and due to these promising results, there are ongoing efforts to create next generation anti-cancer agents by integrating spatial targeting of tumours.

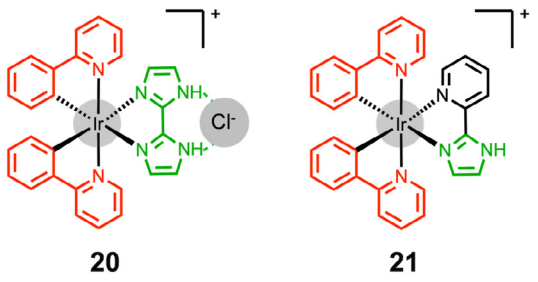


**Fig. 23.** Fluorescent complexes, **20** and **21**, contain an imidazole-based anion binding site (green) and hydrophobic ligands (red) [5]. Hydrogen bonds to chloride anions are shown as green dotted lines.

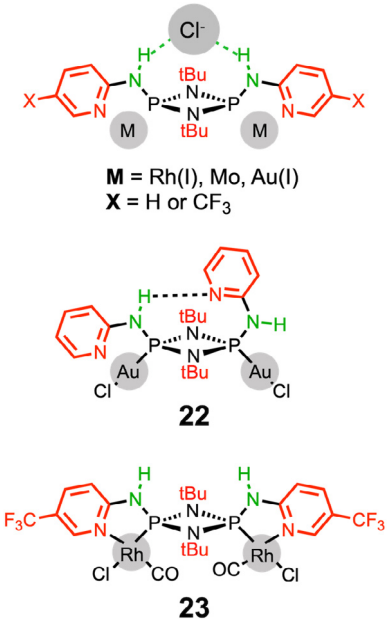


**Fig. 24.** Phosphazane anion transporters contain various chelating (Rh(I), Mo(0)) and non-chelating (Au(I)) metals as well as either H or an electron withdrawing $CF_3$ groups on the pyridine ring. Anion binding groups (green) can either be pointing towards each other, or away from each other. Hydrophobic groups are represented in red [63]. Hydrogen bonds to chloride anions are shown as green dotted lines.

The previous examples show that hydrophobic metal complexes can have potent ion transport activity. Therefore, understanding how to fine-tune the ion binding site can potentially lead to more tailored applications. A report by Wright and co-workers published in 2020 investigated whether anion binding strength can be modulated via coordination chemistry [63]. In this study, metal coordination was applied to alter the conformation of a ligand and lock it in an active conformation with convergent N—H groups for anion chelation, as well as polarizing the N—H groups, thereby making them more potent anion binding sites. Phosphazane ligands were coordinated to a variety of chelating (Rh(I), Mo(0)) and non-chelating (Au(I)) metals, whilst the effect of including an electron withdrawing $CF_3$ moiety into the organic ligand scaffold was also explored (Fig. 24). Overall, the most potent ion transporter of the series was compound **23** shown in Fig. 24, in which the N—H bonds are polarized due to the coordinated Rh(I) cations and the presence of electron withdrawing $CF_3$ groups. The chloride transport activity of the complexes was investigated via the lucigenin quenching assay, which revealed that Rh(I) complexes were more active compared to Mo(0) complexes due to the greater polarization of the NH bond by the more highly charged cation. Furthermore, the chelating metals (Mo(0) and Rh(I)) bound to both the phosphorous and pyridyl-nitrogen atoms of the ligand, effectively locking the ligand in the active conformation, whilst the non-chelated gold complexes were less active, as the metal only coordinated to the phosphorous, allowing free rotation of the P—N bond. The exception to this rule was compound **22** shown in Fig. 24, a gold complex with surprising activity due to anion cap-

ture and release within the coordination sphere of gold seen *via* NMR.

The metals in the previous examples were used for structural reasons, or to polarise or pre-organise the binding site; however, metals can also have roles as responsive modulators of transport activity. As many metals are redox-active, the development of redox-responsive ion carriers is a possible avenue of exploration. One such system was reported by Gale and co-workers in 2020 [20]. In this example, the active anion transporter was based on an organic 1,3-bis(benzi-midazol-2-yl)pyrimidine (BisBzImPy) structure, which was rendered inactive via coordination to gold chloride or gold *N*-heterocyclic carbene, the latter being a more sterically bulky group (BG) to block the binding site of the ligand (complex **24**, Fig. 25). The gold complex **24** was designed to be reduced by glutathione (GSH), a biologically relevant reductant, and subsequent liberation of the organic ligand enables transmembrane chloride transport. A series of complexes were synthesised bearing different electron withdrawing groups at position R in Fig. 25 to polarise the NH chloride binding groups, whilst two different blocking groups (BGs) were explored. Gold chloride was found to be less labile to reduction than the bulkier gold *N*-heterocyclic carbene. These complexes were investigated as cytotoxic agents against cancerous (human colon adenocarcinoma SW620) and non-cancerous (human embryonic kidney HEK293, and human mammary epithelial MCF10A) cell lines, and higher cytotoxic activity was observed in cancer cell lines which is thought to be due to their higher levels of GSH.

As demonstrated by Tecilla and co-workers [62] and Wright and co-workers [63], the coordination sphere of metals can be utilised for the capture and release of anions. Consequently, coordination to target ligands to a metal centre can enable their transport across a bilayer, particularly when binding alters the physical properties such as lipophilicity. Gale and co-workers explore this concept further, reporting a carrier that can bind and transport $OH^-$ ions via coordination to Pt(II) [64]. The carriers are based on square planar platinum triflate complexes (Fig. 26). It is proposed that the labile triflate anion in compound **27** can be displaced by water, and the following deprotonation gives rise to a highly lipophilic platinum hydroxido complex, which is able to partition into the bilayer. Subsequent hydroxide release into the vesicle lumen causes an increase in intravesicular pH which was monitored via the HPTS assay. Interestingly, this carrier can carry out an uphill transport process and establish a transmembrane pH gradient in vesicles ($pH_{in} > pH_{out}$). Additionally, transport was observed against a concentration gradient whereby the external pH was 2 units lower than the internal pH. The $OH^-$ transport activity was also found to be gated by the addition of competing ligands including halides, dihydrogen phosphate, acetate, and nitrate. The authors propose that the anions work by interfering with the hydrolysis of the Pt (II) compounds through ligand exchange reactions.

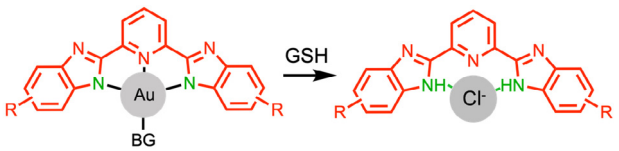


**Fig. 25.** Gold complexes **24** can be reduced by glutathione to release an active chloride ionophore [20]. The NH chloride binding groups are represented in green whilst the hydrophobic groups are represented in red. Hydrogen bonds to chloride anions are shown as green dotted lines.

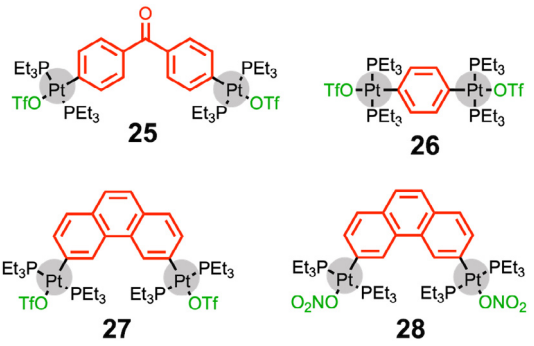


**Fig. 26.** Square planar platinum complexes containing a labile ligand (shown in green) are proposed to hydrolyse in water, and bind $OH^-$ via direct coordination to Pt(II) to give the formation of lipophilic platinum hydroxido complexes [64].

## 4. Conclusions

Metal-organic structures offer unparalleled structural diversity, synthetic facility, and functional flexibility. The field of metal–organic ion transport has great potential to expand to overcome the challenges that lie between design and biological application. This review demonstrates that ion transport can be achieved via the action of a diverse range of metal–organic structures encompassing small carriers, metallocycles, capsules and porous framework materials. To further the field, future work may include exploring more structurally diverse complexes and expanding the functional roles that metals can facilitate. Metals have multifaceted roles in this review as structural components which bring together functional ligands, initiators of self-assembly/disassembly, modulators of transport activity (e.g., redox active modulators), fluorescent complexes for biological imaging applications, and modulators of reactivity.

Future prospects for development in this field are varied and exciting and in this regard the modularity and tunability of metal–organic architectures can be exploited in numerous ways. The structural design of architectures may enable the fine-tuning of interactions with the target guest, whilst screening out others. Similar structural tuning is seen in biology, whereby the potassium channel has a pore just wide enough for potassium, whilst sodium is too small to interact strongly with the channel and cannot be dehydrated [65]. Strides have also been made towards the transport of complex guests such as amino acids *via* the use of chiral cages [61]. Spatial biological targeting may be achieved *via* post-synthetic conjugation with targeting groups such as localizing peptides, antibodies and small molecule targeting groups [24,32]. This will allow better accumulation at the desired site of action. Stimuli responsiveness has been explored in this review, and ultimately, targeted therapeutic effects may be achieved by activating the transporter within disease-specific microenvironments. Alternatively, therapeutic effects may aim to replace the function of a highly regulated biological channel, in which, the activity of the synthetic transporter should ideally be regulated by the same factors that regulate the native channel. The incorporation of fluorescent metals has enabled imaging of transporters, and such innovations could one day lead to the possible combination of imaging and therapy, termed theranostics [25]. It will also be important to understand how to tune biologically relevant parameters in complex models such as bio-distribution, bio-stability, solubility, and off-target toxicity (both derived from the complexes and their component ligands and metal ions).

The funding source(s) had no involvement in the study design; in the collection, analysis and interpretation of data; in the writing of the report; or in the decision to submit the article for publication.

## CRediT authorship contribution statement

**Kylie Yang:** Conceptualization, Writing – original draft, Writing – review & editing. **Hiral A. Kotak:** Conceptualization, Writing – original draft, Writing – review & editing. **Cally J.E. Haynes:** Conceptualization, Writing – original draft, Writing – review & editing.

## Declaration of Competing Interest

The authors declare that they have no known competing financial interests or personal relationships that could have appeared to influence the work reported in this paper. The funding source (s) had no involvement in the study design; in the collection, analysis and interpretation of data; in the writing of the report; or in the decision to submit the article for publication.

## Acknowledgements

CJEH acknowledges financial support from University College London. KY acknowledges funding from EPSRC EP/T025735/1. HK thanks EPSRC for doctoral funding (EP/N509577/1). The authors thank Dr Yang Xu for help in the preparation of Fig. 19.

## References

[1] A.R. Kay, Front. Cell Dev. Biol. 5 (2017) 1–14.
[2] D.C. Gadsby, Nat. Rev. Mol. Cell Biol. 10 (2009) 344–352.
[3] N. Sakai, S. Matile, J. Phys. Org. Chem. 19 (2006) 452–460.
[4] J.T. Davis, P.A. Gale, R. Quesada, Chem. Soc. Rev. 49 (2020) 6056–6086.
[5] M.-H. Chen, Y. Zheng, X.-J. Cai, H. Zhang, F.-X. Wang, C.-P. Tan, W.-H. Chen, L.-N. Ji, Z.-W. Mao, Chem. Sci. 10 (2019) 3315–3323.
[6] L.E. Bickerton, T.G. Johnson, A. Kerckhoffs, M.J. Langton, Chem. Sci. 12 (2021) 11252–11274.
[7] P.A. Gale, J.T. Davis, R. Quesada, Chem. Soc. Rev. 46 (2017) 2497–2519.
[8] N. Akhtar, O. Biswas, D. Manna, Chem. Commun. 56 (2020) 14137–14153.
[9] W. Si, Z.-T. Li, J.-L. Hou, Angew. Chem. Int. Ed. 53 (2014) 4578–4581.
[10] T.M. Fyles, D. Loock, X. Zhou, J. Am. Chem. Soc. 120 (1998) 2997–3003.
[11] C. Goto, M. Yamamura, A. Satake, Y. Kobuke, J. Am. Chem. Soc. 123 (2001) 12152–12159.
[12] X. Wu, J.R. Small, A. Cataldo, A.M. Withecombe, P. Turner, P.A. Gale, Angew. Chem. Int. Ed. 58 (2019) 15142–15147.
[13] M.-M. Russew, S. Hecht, Adv. Mater. 22 (2010) 3348–3360.
[14] A. Kerckhoffs, Z. Bo, S.E. Penty, F. Duarte, M.J. Langton, Org. Biomol. Chem. 19 (2021) 9058–9067.
[15] Y.R. Choi, G.C. Kim, H.-G. Jeon, J. Park, W. Namkung, K.-S. Jeong, Chem. Commun. 50 (2014) 15305–15308.
[16] D. Bléger, J. Schwarz, A.M. Brouwer, S. Hecht, J. Am. Chem. Soc. 134 (2012) 20597–20600.
[17] A.A. Beharry, O. Sadovski, G.A. Woolley, J. Am. Chem. Soc. 133 (2011) 19684–19687.
[18] M. Danial, C.-M.-N. Tran, K.A. Jolliffe, S. Perrier, J. Am. Chem. Soc. 136 (2014) 8018–8026.
[19] N. Busschaert, R.B.P. Elmes, D.D. Czech, X. Wu, I.L. Kirby, E.M. Peck, K.D. Hendzel, S.K. Shaw, B. Chan, B.D. Smith, K.A. Jolliffe, P.A. Gale, Chem. Sci. 5 (2014) 3617–3626.
[20] M. Fares, X. Wu, D. Ramesh, W. Lewis, P.A. Keller, E.N.W. Howe, R. Pérez-Tomás, P.A. Gale, Angew. Chem. Int. Ed. 59 (2020) 17614–17621.
[21] A.J. McConnell, C.S. Wood, P.P. Neelakandan, J.R. Nitschke, Chem. Rev. 115 (2015) 7729–7793.
[22] Y.R. Choi, B. Lee, J. Park, W. Namkung, K.-S. Jeong, J. Am. Chem. Soc. 138 (2016) 15319–15322.
[23] H. Sepehrpour, W. Fu, Y. Sun, P.J. Stang, J. Am. Chem. Soc. 141 (2019) 14005–14020.
[24] A. Casini, B. Woods, M. Wenzel, Inorg. Chem. 56 (2017) 14715–14729.
[25] N. Dey, C.J.E. Haynes, ChemPlusChem 86 (2021) 418–433.
[26] E.G. Percástegui, T.K. Ronson, J.R. Nitschke, Chem. Rev. 120 (2020) 13480–13544.
[27] M.J. Langton, Nat. Rev. Chem. 5 (2021) 46–61.
[28] B. Spyrou, I.N. Hungnes, F. Mota, J. Bordoloi, P.J. Blower, J.M. White, M.T. Ma, P. S. Donnelly, Inorg. Chem. 60 (2021) 13669–13680.
[29] A. Noor, J.K. Van Zuylekom, S.E. Rudd, P.D. Roselt, M.B. Haskali, E. Yan, M. Wheatcroft, R.J. Hicks, C. Cullinane, P.S. Donnelly, Bioconjug. Chem. 32 (2021) 1192–1203.
[30] B.P. Burke, W. Grantham, M.J. Burke, Gary S. Nichol, D. Roberts, I. Renard, R. Hargreaves, C. Cawthorne, S.J. Archibald, P.J. Lusby, J. Am. Chem. Soc. 140 (2018) 16877–16881.
[31] C. He, X. Chen, C.-Z. Sun, L.-Y. Zhang, W. Xu, S. Zhang, Z. Wang, F.-R. Dai, ACS Appl. Mater. Interfaces 13 (2021) 33812–33820.
[32] B. Woods, R.D.M. Silva, C. Schmidt, D. Wragg, M. Cavaco, V. Neves, V.F.C. Ferreira, L. Gano, T.S. Morais, F. Mendes, J.D.G. Correia, A. Casini, Bioconjug. Chem. 32 (2021) 1399–1408.
[33] D.A. Doyle, J.M. Cabral, R.A. Pfuetzner, A. Kuo, J.M. Gulbis, S.L. Cohen, B.T. Chait, R. MacKinnon, Science 280 (1998) 69–77.
[34] T.M. Fyles, C.C. Tong, New J. Chem. 31 (2007) 655–661.
[35] M. Fujita, O. Sasaki, T. Mitsuhashi, T. Fujita, J. Yazaki, K. Yamaguchi, K. Ogura, Chem. Commun. (1996) 1535–1536.
[36] C.P. Wilson, S.J. Webb, Chem. Commun. (2008) 4007–4009.
[37] A.M. Gilchrist, P. Wang, I. Carreira-Barral, D. Alonso-Carrillo, X. Wu, R. Quesada, P.A. Gale, Supramol. Chem. (2021) 1–20.
[38] C.P. Wilson, C. Boglio, L. Ma, S.L. Cockroft, S.J. Webb, Chem. Eur. J. 17 (2011) 3465–3473.
[39] U. Devi, J.R.D. Brown, A. Almond, S.J. Webb, Langmuir 27 (2011) 1448–1456.
[40] J. Kempf, A.R. Schmitzer, Chem. Eur. J. 23 (2017) 6441–6451.
[41] A. Kadej, M. Kuczer, E. Czarniewska, A. Urbański, G. Rosiński, T. Kowalik-Jankowska, J. Inorg. Biochem. 163 (2016) 147–161.
[42] L.M. Gaetke, C.K. Chow, Toxicology 189 (2003) 147–163.
[43] W.-Y. Gao, R. Cai, T. Pham, K.A. Forrest, A. Hogan, P. Nugent, K. Williams, L. Wojtas, R. Luebke, Ł.J. Weseliński, M.J. Zaworotko, B. Space, Y.-S. Chen, M. Eddaoudi, X. Shi, S. Ma, Chem. Mater. 27 (2015) 2144–2151.
[44] M.M. Tedesco, B. Ghebremariam, N. Sakai, S. Matile, Angew. Chem. Int. Ed. 38 (1999) 540–543.
[45] M. Jung, H. Kim, K. Baek, K. Kim, Angew. Chem. Int. Ed. 47 (2008) 5755–5757.
[46] M. Eddaoudi, J. Kim, J.B. Wachter, H.K. Chae, M. O'Keeffe, O.M. Yaghi, J. Am. Chem. Soc. 123 (2001) 4368–4369.
[47] H. Furukawa, J. Kim, K.E. Plass, O.M. Yaghi, J. Am. Chem. Soc. 128 (2006) 8398–8399.
[48] O.V. Kulikov, R. Li, G.W. Gokel, Angew. Chem. Int. Ed. 48 (2009) 375–377.
[49] A.D. Peters, S. Borsley, F. della Sala, D.F. Cairns-Gibson, M. Leonidou, J. Clayden, G.F.S. Whitehead, I.J. Vitórica-Yrezábal, E. Takano, J. Burthem, S.L. Cockroft, S.J. Webb, Chem. Sci. 11 (2020) 7023–7030.
[50] T. Koshiyama, Y. Inoue, S. Asada, K. Kawahara, S. Ide, K. Yasuhara, M. Ohba, Chem. Commun. 57 (2021) 2895–2898.
[51] A. Satake, M. Yamamura, M. Oda, Y. Kobuke, J. Am. Chem. Soc. 130 (2008) 6314–6315.
[52] C.J.E. Haynes, J. Zhu, C. Chimerel, S. Hernández-Ainsa, I.A. Riddell, T.K. Ronson, U.F. Keyser, J.R. Nitschke, Angew. Chem. Int. Ed. 56 (2017) 15388–15392.
[53] Y. Li, L. Jia, X. Tang, J. Dong, Y. Cui, Y. Liu, Mater. Chem. Front. 6 (2022) 1010–1020.
[54] M. Boccalon, E. Iengo, P. Tecilla, J. Am. Chem. Soc. 134 (2012) 20310–20313.
[55] L.J. Lalgee, L. Grierson, R.A. Fairman, G.E. Jaggernauth, A. Schulte, R. Benz, M. Winterhalter, Biochim. Biophys. Acta, Biomembr. 2014 (1838) 1247–1254.
[56] E. Mahon, S. Garai, A. Müller, M. Barboiu, Adv. 27 (2015) 5165–5170.
[57] R. Kawano, N. Horike, Y. Hijikata, M. Kondo, A. Carné-Sánchez, P. Larpent, S. Ikemura, T. Osaki, K. Kamiya, S. Kitagawa, S. Takeuchi, S. Furukawa, Chem 2 (2017) 393–403.
[58] H. Wang, X. Qian, K. Wang, M. Su, W.-W. Haoyang, X. Jiang, R. Brzozowski, M. Wang, X. Gao, Y. Li, B. Xu, P. Eswara, X.-Q. Hao, W. Gong, J.-L. Hou, J. Cai, X. Li, Nat. Commun. 2018 (1815) 9.
[59] S.M.N. Uddin, S. Laokroekkiat, M.A. Rashed, S. Mizuno, K. Ono, M. Ishizaki, K. Kanaizuka, M. Kurihara, Y. Nagao, T. Hamada, Chem. Commun. 56 (2020) 1046–1049.
[60] D.P. August, S. Borsley, S.L. Cockroft, F. della Sala, D.A. Leigh, S.J. Webb, J. Am. Chem. Soc. 142 (2020) 18859–18865.
[61] Y. Li, J. Dong, W. Gong, X. Tang, Y. Liu, Y. Cui, Y. Liu, J. Am. Chem. Soc. 143 (2021) 20939–20951.
[62] D. Milano, B. Benedetti, M. Boccalon, A. Brugnara, E. Iengo, P. Tecilla, Chem. Commun. 50 (2014) 9157–9160.
[63] A.J. Plajer, J. Zhu, P. Pröhm, F.J. Rizzuto, U.F. Keyser, D.S. Wright, J. Am. Chem. Soc. 142 (2020) 1029–1037.
[64] L.-J. Chen, X. Wu, A.M. Gilchrist, P.A. Gale, Angew. Chem. Int. Ed. 61 (2022) e202116355.
[65] I.H. Shrivastava, D. Peter Tieleman, P.C. Biggin, M.S.P. Sansom, Biophys. J. 83 (2002) 633–645.